LA-UR -85-1652

RECEIVED BY OSTI JUN 07 1985

CONF-850504--133

LA-UR--85-1652

DE85 012708

TITLE TIME-RESOLVED CURRENT, CURRENT-DENSITY, AND EMITTANCE MEASUREMENTS OF THE PHERMEX ELECTRON BEAM

AUTHOR(S) D. C. Moir, L. A. Builta, and T. P. Starke

SUBMITTED TO IEEE, 1985 Particle Accelerator Conference, Vancouver, B.C., Canada, May 13-16, 1985

Los Alamos Los Alamos National Laboratory Los Alamos, New Mexico 87545

FORM NO 836 R4
ST NO 2629 5/81

DISTRIBUTION OF THIS DOCUMENT IS UNLIMITED

TIME-RESOLVED CURRENT, CURRENT-DENSITY, AND EMITTANCE MEASUREMENTS OF THE PHERMEX ELECTRON BEAM

D. C. Moir, L. A. Builta, and T. P. Starke
Los Alamos National Laboratory
P. O. Box 1663, MS P940
Los Alamos, New Mexico 87545

Introduction

The PHERMEX electron-beam pulse is a burst of ten 3.3-ns micropulses separated by 20 ns. Typical accelerator operating parameters produce a mean beam micropulse energy of 26 MeV with peak current of 300-500 A. A description of the facility is given in Refs. [1] and [2]. The purpose of this work is to present experimental measurements of the current, current density, and emittance of a single PHERMEX micropulse.

This experiment is part of an effort to completely characterize the PHERMEX electron beam. Understanding the electron-beam parameters is necessary for machine upgrade as related to flash radiography and for both present and future electron-beam experiments. Additional details of this experiment are available in Ref. [3].

Concept

Electrons ejected from the 50-MHz accelerating cavities are transported through 9.5 m of drift space before they are focused onto an x-ray converter. Beam transport and focusing are accomplished using two solenoidal focusing lenses and one steering-lens dipole pair. One focusing lens (collimating lens) is located at the end of the last accelerating cavity. The other (final-focusing lens) is 0.5 m from the exit of the PHERMEX drift space. For typical accelerator operation, the collimating lens and steering magnet are tuned to produce a 10-mm-radius beam at the entrance of the final-focusing lens. The final-focusing lens is used to produce a minimum beam radius (~1 mm) at the exit of the accelerator drift tube.

For flash radiography the focused beam exits a 0.5-mm-thick beryllium window and impinges on a 1.75-mm-thick tungsten target producing a 26-MeV bremsstrahlung gamma spectrum. In electron-beam-propagation experiments this same focused beam is extracted through the beryllium window into a gas-filled experimental chamber. Experiments studying the emittance of this beam after extraction through the beryllium foil indicate that the emittance is dominated by multiple scattering in the beryllium window. Understanding the character of the beam upstream of the beryllium window is extremely important. The beam at the exit of the beryllium is very close to the shape of the beam in vacuum because the Coulomb multiple scattering has not changed the radial size of the beam. By examining the vacuum expansion of the unscattered beam downstream of the collimator we can extrapolate back to the exit of the collimator to determine the beam structure at the exit of the beryllium foil.

Experiment

The hardware for performing these measurements was set up outside of the PHERMEX chamber. The bullnose and the front panel of the protective envelope were removed to expose the end of the PHERMEX drift tube. Figure 1 is a schematic of the hardware assembly. The standard 3-mm-exit-diam tapered collimator (4°) was replaced with a 10-mm-exit-diam aluminum collimator with a 4° taper. The beryllium vacuum window was removed from the end of the collimator. A 305-mm-diam brass drift tube was attached to the PHERMEX beam line with an adaptor flange. The vacuum drift space was 750 mm long and contained an insertable tungsten emittance mask. The mask was located 500 mm from the end of the collimator. Figure 2 is a schematic of the mask. The 25-MeV electron range for tungsten is 10.4 g/cm^2, or 5.4-mm thickness using density of 19.3 g/cm^3 for tungsten. The mask used in the experiment was 5.3 mm thick. The slot size (1.58 mm) and spacing (5 mm) were chosen by assuming a symmetric beam at the exit of the collimator with a diameter of 1 mm and a divergence half angle of 20 mrad. With these conditions, the beam diameter at the emittance mask (500 mm from the collimator) is 20 mm, and the finite thickness effects of the mask slots are approximately 10% of the slot width of 1.5 mm.

The vacuum drift chamber was capped with a 25.4-mm-thick aluminum end plate. The center of the end plate was machined to create a 3.0-mm-thick, 100 mm-diam window along the beam axis. A 0.125-mm-thick Kapton foil was placed on the outside of the thinned aluminum plate. A 100-mm-diam, 6.35-mm-thick front-surface turning mirror for imaging light from the Kapton foil was placed in the beam line. The mirror was centered and rotated 45° relative to the beam axis. A 75-mm-thick aluminum charge collector was located just downstream of the mirror. The Kapton foil, mirror, and charge collector were all at 580-torr air.

Diagnostics for the experiment produced time-resolved electrical and optical signals. The beam current was monitored by a Faraday cup and the self-integrated azimuthal magnetic-sense (B-dot) loops in the vacuum drift section (Fig 1). Each of the signals was divided so that it could be monitored on a fast sweep using a Tektronix 7104 oscilloscope (1 ns/div or 10 ns/div) and a Tektronix 7912 transient digitizer (30 ns/div).

An Imacon Model 675 electronic streak/frame camera was used for imaging Cerenkov light from the Kapton foil [4]. The camera is triggered 100 ns before the electron beam. The trigger system has an rms trigger jitter of ±20 ns. As a consequence, the absolute time of the streak-camera trigger relative to the electron beam and internal camera delay is essential information for determining the micropulse number that is on the film. This is especially important for fast streak speeds.

The transfer optics from the Kapton foil to the slit plane consisted of the front-surface mirror described earlier and an f-1.2, 152-mm-focal-length lens mounted on the Imacon 675 camera. The interior of the air drift space containing the mirror and charge collector was painted flat black to absorb stray light and reflections. A cardboard tube was inserted between the lens and the drift-tube port to eliminate external light.

Shot M13 is a typical 2.6-ns/mm, open-slit, streak-camera record (Fig. 3) with the emittance mask removed. Several qualitative features should be noted. First, the 5-mm ink-grid lines on the Kapton are clearly evident. This not only gives a scale for the measurement but also yields a reference for locating the slit when the streak measurements are to be made, that is, the slit can be placed precisely through the center of the beam. Each beam micropulse is different, even though they have approximately the same current amplitude as measured by the Tektronix 7912 record. Finally, the beam is hollow with an asymmetric core in the center.

A microdensitometer (100-μm scan aperture) was used to digitize the data on Shot M13. The film density of each of the pulse images was averaged in time, and the resulting average peak film density above fog was compared with the measured currents. The net film density increases with beam current; however, the relationship is not linear and, in fact, appears to saturate. Unfortunately, there are insufficient data to obtain an exposure curve. Pulses 2-4 indicate that this film-density measurement is accurate to about 10%.

With the open-slit photographs of the beam and grid as a reference, the 0.1-mm slit was located at the center of beam distribution. Streak measurements of the center of the electron beam were made. The photographic reproduction of a single pulse record with 0.45-ns/mm streak-camera speed is shown in Fig. 4 (Shot T46). This result indicates that the front of the electron beam is hollow with a solid core at the end of the micropulse. The tail of the beam ends abruptly and flares in one direction.

This record was also scanned with the microdensitometer (100-μm aperture), and the film-density distribution was averaged over the entire spatial coordinate of the micropulse. The result is a two-dimensional plot of average film density vs time. This can be compared with the beam current measured by the self-integrated B-dot loops. A comparison of the average film density and the self-integrated B-dot loop indicates that the shape of the optical signal is the same as the B-dot loop. Each has a slow risetime and a fast decay. However, quantitative comparison of the two indicates that the optical signal is [illegible] ns wide at the base where the electronic signal is [illegible] ns long. This discrepancy is most probably due to recently observed transient darkening of the Kapton during the electron-beam pulse.

The final streak-camera configuration was with the emittance mask inserted in the beam path. These data were taken with and without the 0.1-mm slit in the camera. Figure 5 (Shot T47) is a sample of a measurement with 0.1-mm slit. The data taken without the slit are not as useful because signal integration reveals large variations in emittance. The design of the slotted mask was based on divergence and spot-size experiments with the beryllium windows. Unfortunately, it was inadequate for measuring the cold, small-diameter beam that we observed in this experiment. Experimental analysis of these data is useful for obtaining limits or bounds on the beam emittance. The film was scanned with a microdensitometer using a [illegible]-μm aperture.

The resulting scan of Fig. 5 can be used to obtain an estimate of the electron-beam emittance at the core of the beam where we have the peak current and current density. The following assumptions are made to obtain an emittance plot and emittance value: (1) the beam temperature at the edge of the beam is zero, (2) maximum beam divergence occurs at the edge of the beam, (3) the beam temperature is defined for the center of the beam, and (4) the beam divergence is used to estimate the beam radius at [illegible]-mm axial position. The unnormalized emittance at peak current obtained from the above assumptions is approximately [illegible] mm mrad and is clearly an upper bound estimated with limited data. The normalized emittance is [illegible] mm mrad.

Conclusions

The normalized emittance of the beam injected into PHERMEX has been measured [5] and is 240π mm mrad. This agrees well with our estimated normalized emittance of 260π mm mrad. In addition, the peak injected current [5] was 450 A, and the transported peak current measured for this report was 400 A. The above results indicate that most of the peak beam current is transported through PHERMEX without significant emittance growth.

The summary of the time-resolved data indicates that the beam is hollow in the front and is solid at the peak current near the end of the pulse. The beam radius at an axial location of 778 mm increases from near zero at the front of the pulses to a peak of 8 mm where the beam is hollow. The beam then necks down to a minimum of 3.8 mm at peak current and finally flares out on the end to an 8-mm radius. The divergence follows the radius, that is, peak divergence occurs at peak radius. The average 1-eV beam temperature is constant over the entire pulse. The beam current has a slow risetime, peaks at approximately 400 A, then falls rapidly.

Clearly, the beam is not cylindrically symmetric in space and it may not be symmetric in time, but these assumptions are necessary to present data that will be useful for calculations using one- and two-dimensional transport and propagation codes. The fact that the beam is not symmetric is of concern, but an accurate description of the asymmetry would require special study.

The beam was much colder than expected, and the emittance mask was therefore too coarse. A future experiment would require much more narrow slot spacing and width. The emittance mask was much thicker than necessary. Only sufficient material thickness to scatter the beam is required. The recorded signal could still be distinguished from the background produced by the scattered beam. Finally, the Kapton foil needs to be replaced by a detector that is not subject to transient darkening when irradiated.

The fact that the beam is hollow in front is surprising and disturbing. Both radiographic performance as well as the beam-propagation applications of the facility are affected. The hollow beam tends to increase the effective radiographic beam spot size, which is undesirable for hydrodynamic experiments requiring large magnifications. It is also undesirable for beam propagation because hollow beams tend to promote filamentation instabilities. These are undesirable for beam propagation. While the cause of the hollowing is unknown at present, there is speculation that it is produced by space-charge effects in the first cavity.[4] Verification would require additional experiments and calculations.

References

[1] D. Venable, [illegible] Dickman, J. N. Hardwick, E. D. Bush, Jr., R. W. Taylor, T. J. Boyd, J. R. Ruhe, E. J. Schneider, B. T. Rogers, and H. G. Worstell, "PHERMEX: A Pulsed High-Energy Radiographic Machine Emitting X-rays," Los Alamos Scientific Laboratory report LA-3241 (May 1967).

[2] T. P. Starke, "PHERMEX Standing-Wave Linear Electron Accelerator," IEEE Trans. Nucl. Sci., Vol. NS-30 (2), 1402 (1983).

[3] P. J. Moir, L. A. Builta, and T. P. Starke, Los Alamos National Laboratory document M-4:GR-84-6 (1984).

[4] J. Clark, Lawrence Livermore National Laboratory, personal communication, June 1984.

[5] L. A. Builta, J. C. Elliott, D. C. Moir, T. P. Starke, and C. A. Vecere, "PHERMEX Electron-Gun Development," IEEE Trans. Nuc. Sci., Vol. NS-30 (4), 2728 (1983).

[6] Brendan Godfrey, Mission Research Corporation, personal communication, January 1984.

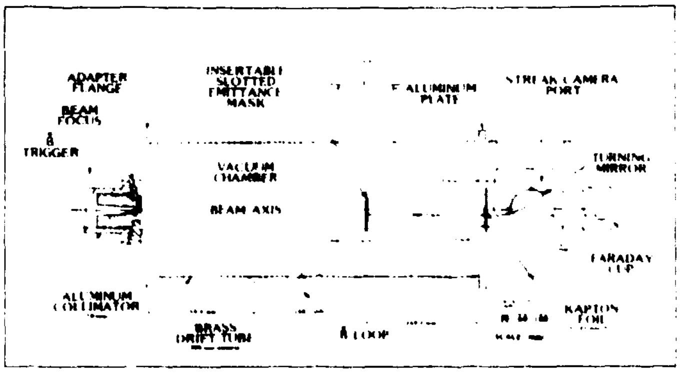

Fig. 1. Schematic of drift-tube arrangement.

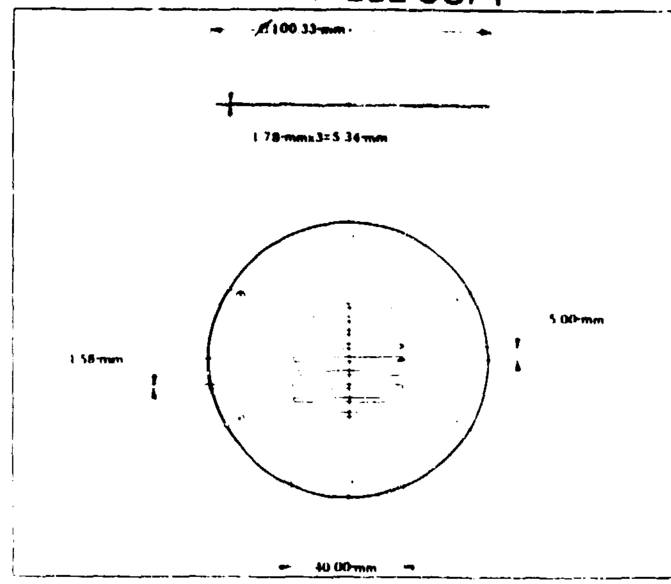

Fig. 2. Tungsten emittance mask.

Fig. 3. Shot M13 open-shutter streak-camera record.

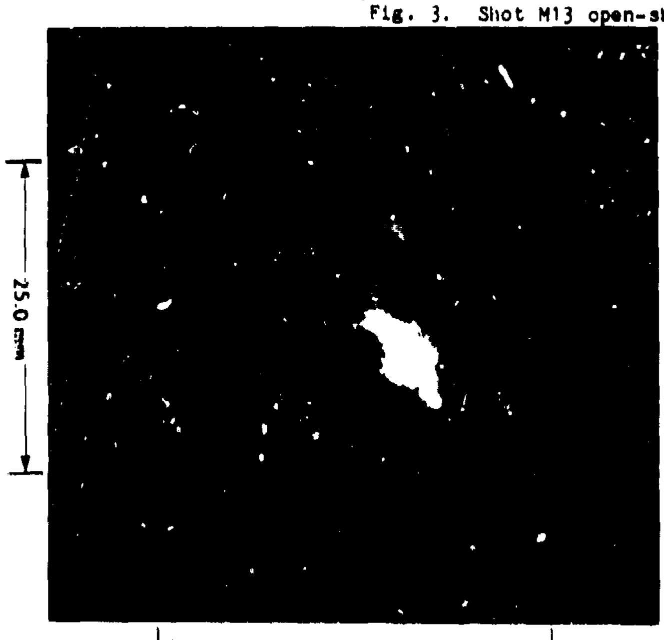

Fig. 4. Shot T46 streak-camera record of a single micropulse.

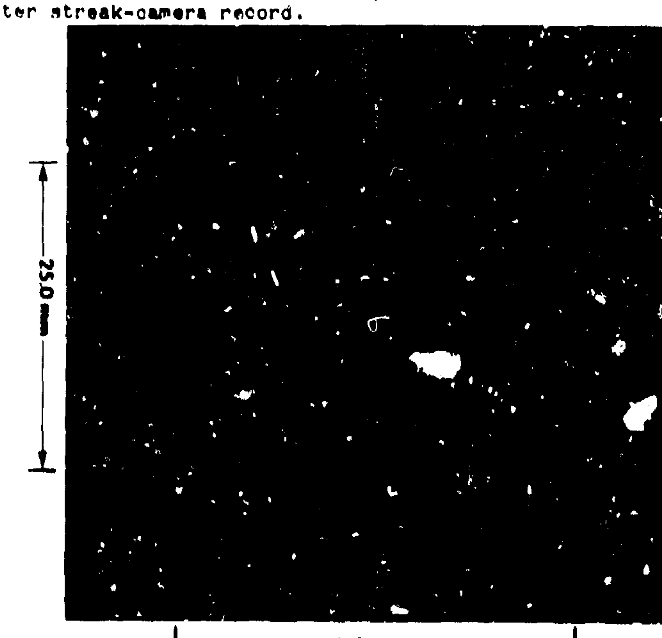

Fig. 5. Shot T43 streak-camera record of a single micropulse with the emittance mask inserted.